Since January 2020 Elsevier has created a COVID-19 resource centre with free information in English and Mandarin on the novel coronavirus COVID-19. The COVID-19 resource centre is hosted on Elsevier Connect, the company's public news and information website.

Respir. Med and Res 80 (2021) 100862

Available online at
ScienceDirect
www.sciencedirect.com

Elsevier Masson France
EM|consulte
www.em-consulte.com

Letter to the Editor

Two-photon microscopy analysis reveals different pulmonary damage after infection by influenza or SARS-CoV-2

ARTICLE INFO

Article history:
Received 23 August 2021
Accepted 21 September 2021
Available online 2 October 2021

Keywords:
2-photon microscopy
Influenza
COVID-19

Dear Editors,—COVID-19 and influenza have different epidemiology and clinical features [1–3] but histological data has indicated that both cause same epithelial lesions and diffuse alveolar damage [4]. To investigate these pandemic respiratory system viruses we used 2-photon microscopy (2PM) on animal model to compare structural lung damage, viral localization and macrophage recruitment in pulmonary epithelial tissue 72 h after infection with either the *A/PR8 Influenza* strain infection in mice or *SARS-Cov-2* infection in hamsters. The use of 2PM enabled the visualization of a thick section of an entire lung while maintaining excellent resolution.

Methods

The method section has been divided into sub-parts describing animals, viruses, infection modalities and antibodies used for each virus.

For *Influenzavirus* infection,

Mice. Six- to 8-week old male transgenic mice (C57BL/6 background) expressing yellow fluorescent protein (YFP) under the control of the CD11c promoter (a kind gift of Dr. Lefevre F., Molecular Immunology and Virology Unit, Institut National de la Recherche Agronomique, Jouy en Josas, France) called CD11c-YFP mice. Mice were handled under specific pathogen-free conditions.

Influenzavirus

A/Puerto Rico/8/34/H1N1, which express a fluorescent protein (Red Fluorescent Protein (RFP)) fused to the NS1 protein (RFP-NS1-PR8), were generated previously by using reverse genetics.

For *SARS-Cov2* infection,

Hamster. Male Syrian hamsters (*Mesocricetus auratus*) of 5-6 weeks of age were purchased from Janvier Laboratories and handled under specific patho-gen-free conditions (a kind gift of Dr. Dias de Melo G., Lyssavirus Epidemiology and Neuropathology Unit, Institut Pasteur, Paris, France).

SARS-Cov2

The strain 2019-nCoV/IDF0372/2020 (EVAg collection, Ref-SKU: 014V-03890) was provided by Pr. Van der Werf S. (Institut Pasteur, Paris).

Infection protocol

Three mices were anesthetized with 5% isoflurane and were intranasally infected with 10^5 PFUs (plaque-forming units) of RFP-NS1-PR8. Three hamsters were anesthetized with 5% isoflurane and were intranasally infected with 6.104 PFUs of SARS-CoV-2. For both species, 1 Mock-infected animals received the physiological solution only with the same procedure. Infected and mock-infected animals were housed in separated isolators for each species and all animals were followed-up daily with body weight and clinical score.

At day 3 post infection, mices and hamsters (infected and mock) were euthanized by cervical dislocation, prepared with intracardiac perfusion of 10 ml PBS then 10 ml 4% Paraformaldehyde (PFA) solution. After lung harvesting, left lobe was glued on Vibratome® stage (Leica, Wetzlar, Germany) and immersed in PBS. In order to achieve smooth sectioning of lung, lung was cut in two parts at 10 μm/s with vibration amplitude of razor blade of 3 mm. Lower section (4 mm thick) was glued on 83mm Petri dish and immersed in PBS for imaging.

We chose day 3 post infection because hamsters had lost 25% weight (ethical endpoint), so we compared with mice infected at the same day post infection.

Immunofluorescence staining protocol was described in legend of each figure.

For both species, infected and mock-infected lung sections have followed the same experimental protocol.

https://doi.org/10.1016/j.resmer.2021.100862

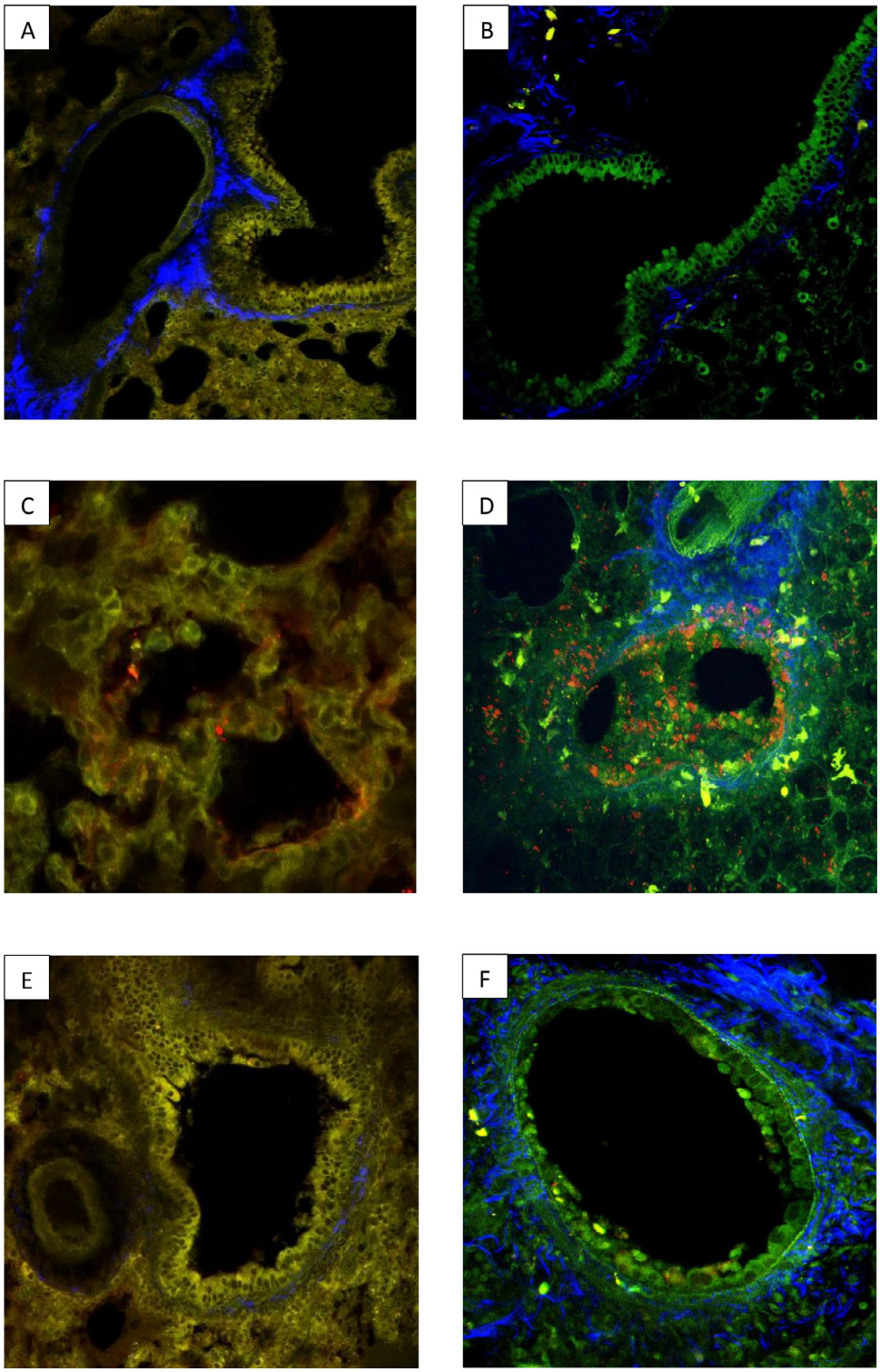

Fig. 1. Comparative analysis with 2MP of lung injury after infection with *SARS-Cov2* or *Influenzavirus*. The images above show two 2-photon micrographs (2PM) of normal hamster (A) and mouse (B) lung parenchyma. Alveolar/bronchial epithelium tissue is shown in yellow (A) or green (B) and connective tissue (in both micrographs) is blue. Two 2PM micrographs of pulmonary parenchyma showing the distribution of SARS-Cov-2 (C) or the A/PR8 influenza (D) virus 72 h after infection. In (C) the hamster tissue was stained with the SARS-Cov-2 Spike antibody and a secondary antibody coupled with AF568, an orange-red dye. In (D) the mouse tissue was stained with an endogen fluorescence NS1 coupled with a red fluorescent marker (RFP). The images show that SARS-CoV-2 was localized exclusively on the alveolar epithelium whereas the influenza virus was predominantly localized the on bronchial and alveolar epithelia. Two 2PM micrographs of pulmonary bronchial epithelia 72 h after infection with either SARS-Cov-2 (E) or A/PR8 influenza (F) virus. In (E) the hamster tissue was stained with the SARS-Cov-2 Spike antibody and a secondary antibody coupled with AF568, an orange-red dye. In (F) the mouse tissue was stained with an endogen fluorescence NS1 coupled with a red fluorescent marker (RFP) to visualise the influenza virus. The bronchial epithelium (E) had a normal structure 72 h following infection with Sars-Cov-2 in contrast to the epithelium (F) which showed signs of severe injury following infection with *Influenzavirus*.

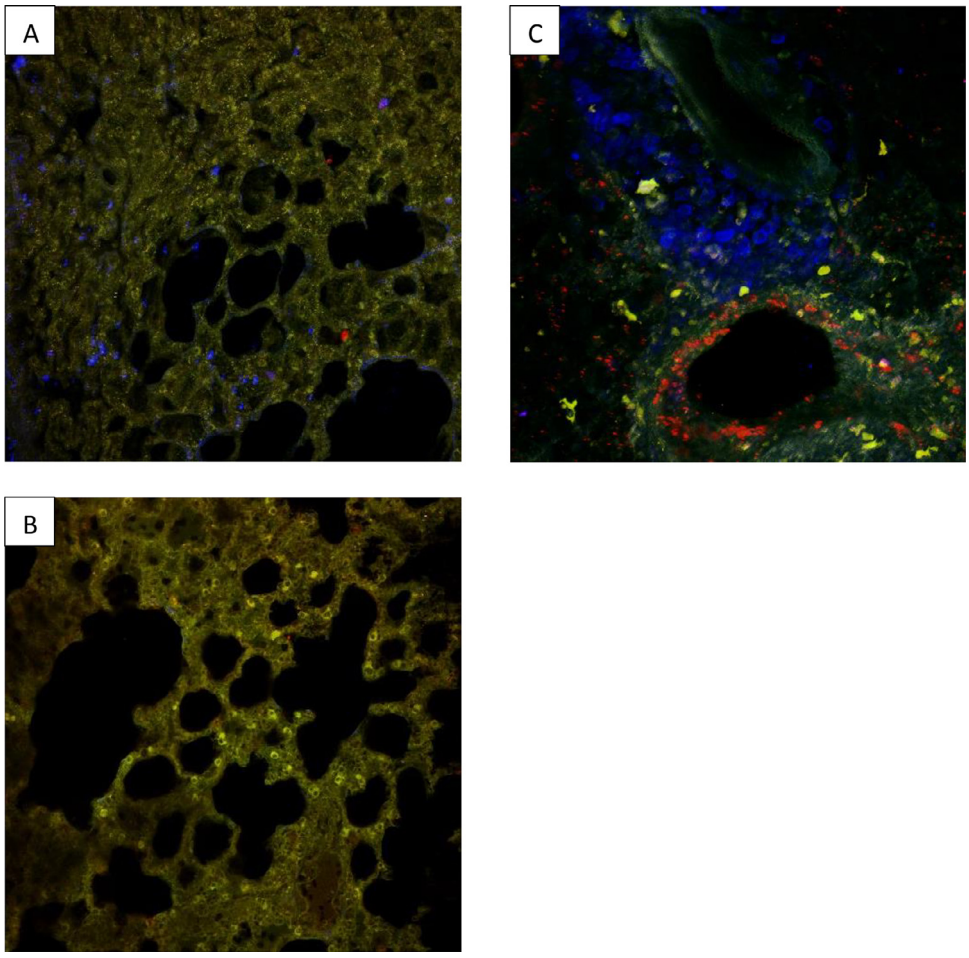

Fig. 2. Comparison of three 2PM images showing localized macrophage recruitment in pulmonary epithelial tissue 72 h after infection with either SARS-Cov-2 virus (A) and (B), or A/PR8 influenza (C). In all slides an F4/80 antibody coupled with a blue BV421 fluorescent marker was used to stain the macrophages. In slides (A) and (B) the SARS-Cov-2 Spike antibody and a secondary antibody coupled with AF568 (an orange-red dye) were used to stain the SARS-Cov-2 virus and in slide (C) an endogenous, fluorescent NS1 coupled with a red fluorescent marker (RFP) were used to visualise the influenza virus. Macrophage recruitment in SARS-Cov-2 infected lungs was heterogenous, with diseased (A) and healthy areas (B) in the same organ. This variation in macrophage distribution differed from the general, diffuse macrophage recruitment from the perivascular area observed in lung tissue after infection with influenza (C).

Ethics

All animal care and experiments conformed to the guidelines for animal experiments of the European legislation about animal experimentation, and were approved by the animal research committee of Institut de Recherche Biomédicale des Armées.

Two-photon microscopy

The intravital imaging was performed by using an LSM 780 NLO (Carl Zeiss) equipped with an infrared laser (Chameleon; Coherent). To acquire images, the wavelength of the first laser was set to 1100 nm for excitation of RFP and AF568. The wavelength of the second laser was set to 850 nm for excitation to YFP, second harmonic and BV421. Each lung section of infected and mock-infected animals of both species was fully explored by microscopy to map of affected areas.

Results

The results have been illustred and described on Figs. 1 and 2 and their legends (above). M2P has clearly highlighted several differences between 2 viruses about viral localization, repartition and localization of pulmonary damage and macrophage recruitment.

To have physiological references, the Fig. 1 showed normal lung parenchyma without infection of mock-infected hamster (A) and mock-infected mice (B).

After infection, the Fig. 1 showed that *SARS-Cov2* was localized within alveolar epithelium (C) while *Influenzavirus* was mainly bronchial (D). This figure also showed bronchial epithelium integrity was preserved during a *SARS-CoV-2* infection (E) but destroyed by *Influenzavirus* (F).

The Fig. 2 showed that infection with *SARS-CoV-2* induced focal damage and focal macrophage infiltration, resulting patches of healthy (B) and diseased tissue (A). While infection with *Influenzavirus* caused diffuse, homogenous lung damage and diffuse macrophage recruitment from the perivascular area (C).

In conclusion, SARS-Cov-2 and Influenzavirus are both respiratory viruses with microscopic pathophysiological differences. This could help to explain their observed clinical differences and the need for different therapeutic approaches. M2P could explain some physiopathological difference: bronchial integrity after SARS-Cov2 infection could be one of explanation of less risk of bacterial infectious complication comparatively with important risk due to epithelium damage after influenza infection. 2MP appears to be promising tool for exploring viral pathophysiology, comparing respiratory viruses and testing therapeutic strategies in preclinical stage.

Declaration of Competing Interest

None.

The images have not been previously published.

CRediT authorship contribution statement

Frédéric Rivière: Conceptualization, Data curation, Formal analysis, Writing – original draft. **François Lefèvre:** Writing – review & editing. **Julien Burger:** Writing – review & editing. **Guilherme Dias de Melo:** Writing – review & editing. **Jean Nicolas Tournier:** Writing – review & editing. **Emmanuelle Billon-Denis:** Conceptualization, Data curation, Formal analysis, Writing – review & editing.

Funding

None.

References

[1] Salata C, Calistri A, Parolin C, Palù G. Coronaviruses: a paradigm of new emerging zoonotic diseases. Pathog Dis 2019;77:ftaa006. 1 déc.
[2] Piroth L, Cottenet J, Mariet AS, Bonniaud P, Blot M, Tubert-Bitter P, et al. Comparison of the characteristics, morbidity, and mortality of COVID-19 and seasonal influenza: a nationwide, population-based retrospective cohort study. Lancet Respir Med 2021;9:251–9 mars.
[3] Erich P, Mario K, Theresa M, Sara O, Hasan K, Sebastian B, et al. COVID-19 is not "just another flu": a real-life comparison of severe COVID-19 and influenza in hospitalized patients in Vienna, Austria. Infection 2021;49(5):907–16. doi:10.1007/s15010-021-01610-z.
[4] Hariri LP, North CM, Shih AR, Israel RA, Maley JH, Villalba JA, et al. Lung histopathology in coronavirus disease 2019 as compared with severe acute respiratory sydrome and H1N1 influenza. Chest 2021;159:73–84 janv.

Frédéric Rivière*
François Lefèvre
Julien Burger
Guilherme Dias de Melo
Jean Nicolas Tournier
Emmanuelle Billon-Denis
Microbiology and Infectious Diseases Department, Institut de Recherche Biomédicale des Armées, Place Générale Valérie André, Brétigny-sur-Orge 91220, France
Respiratory Department, Hôpital d'Instruction des Armées Percy, Clamart 92140, France
Molecular Immunology and Virology Unit, Institut National de la Recherche Agronomique, Domaine de Vilvert, Jouy-en-Josas Cedex 78352, France
Lyssavirus Epidemiology and Neuropathology Unit, Institut Pasteur, Paris 75015, France

*Corresponding author at: Microbiology and Infectious Diseases Department, Institut de Recherche Biomédicale des Armées, Place Générale Valérie André, Brétigny-sur-Orge 91220, France.
E-mail address: frdriviere@orange.fr (F. Rivière).

Received 23 August 2021
Revised 15 September 2021
Accepted 21 September 2021

Available online 2 October 2021